

Current Topics

Design of Photoactive Ruthenium Complexes To Study Interprotein Electron Transfer[†]

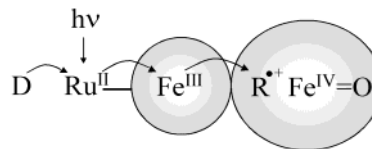
Francis Millett* and Bill Durham

Department of Chemistry and Biochemistry, University of Arkansas, Fayetteville, Arkansas 72701

Received June 13, 2002; Revised Manuscript Received July 24, 2002

Electron-transfer reactions play essential roles in numerous important biological processes, including photosynthesis, mitochondrial respiration, and intermediary metabolism. Kinetic characterization of biological electron-transfer reactions has proven to be a formidable task because the rate constants are often very large. Relatively few techniques have been developed to measure rapid electron transfer between redox centers within a protein complex. These techniques include pulse radiolysis (1) and flash photolysis methods utilizing photosynthetic reaction centers (2), metal-substituted porphyrins (3), flavins (4), thiouredopyrenetrisulfonate (5), and CO-bound heme proteins (6). We have introduced a new method to study intracomplex electron transfer that utilizes a photoactive tris(bipyridine)ruthenium group [Ru(II)] which is covalently attached to a protein such as cytochrome *c* (Scheme 1) (7). Photoexcitation of Ru(II) to the metal-to-ligand charge-transfer state, Ru(II*), a strong reducing agent, leads to rapid electron transfer to the ferric heme group in cytochrome *c* (Cc).¹ Subsequent electron transfer from photoreduced heme *c* to redox center(s) in the other protein can be measured on a time scale as fast as 50 ns. This technique has been used to measure intracomplex electron transfer between cytochrome *c* and its physiological partners,

Scheme 1



cytochrome *c* oxidase (8–12), cytochrome *bc*₁ (13–15), cytochrome *c* peroxidase (16–24), and cytochrome *b*₅ (25, 26). In this review, we will discuss the design of ruthenium complexes for efficient photoinitiation of electron transfer, and their use for studying intracomplex electron transfer.

DESIGN OF RUTHENIUM COMPLEXES FOR PHOTOINITIATION OF ELECTRON TRANSFER

Gray and co-workers (27) and Isied et al. (28) introduced the use of tethered ruthenium complexes by specifically attaching a Ru(NH₃)₅ complex to His-33 of cytochrome *c*. Since the resulting Ru(NH₃)₅(His) complex is not itself photoactive, an external reducing agent was used to initiate electron transfer between the ruthenium and heme groups. Our laboratory introduced four different strategies for specifically labeling proteins with photoredox-active ruthenium polypyridyl complexes. In methods 1 and 2, a lysine amino group is labeled with a ruthenium reagent containing a reactive *N*-hydroxysuccinamide ester (7, 29) or bromomethyl group (30), respectively. Method 3 involves the reaction of Ru(bpy)₂(H₂O)₂²⁺ with a surface histidine, followed by reaction with imidazole to form Ru(bpy)₂(imidazole)(His)-Cc (31, 32). We discovered that this ruthenium complex can be photoexcited to the redox-active Ru(II*) state (32). Gray

[†] This work was supported by NIH Grants GM20488 and NCR R COBRE 1 P20 RR15569.

* To whom correspondence should be addressed. Phone: 479-575-4999, FAX: 479-575-4049, E-mail: millett@uark.edu.

¹ Abbreviations: Cc, cytochrome *c*; hCc, horse Cc; yCc, yeast iso-1-Cc; CcP, cytochrome *c* peroxidase; CcO, cytochrome oxidase; 2Fe₂S, Rieske iron-sulfur center; Ru-39-Cc, Ru(bpy)₂dmb-Cys-39-(H39C;C102T)-yCc; bpy, 2,2'-bipyridine; dmb, 4,4'-dimethyl-2,2'-bipyridine; bpz, 2,2'-bipyrazine; bphb, 1,4-bis(2,2'-bipyridyl-4'-yl)-benzene; qpy, 2,2':4',4'':2'',2'''-quaterpyridine.

and co-workers developed a method to convert Ru(II*) to Ru(III) using sacrificial oxidants (33) and have used this complex extensively in electron-transfer studies (34, 35). In method 4, the sulfhydryl group of a protein cysteine residue is labeled with a ruthenium reagent containing a bromomethyl group (9, 16, 25). A major advantage of method 4 is that the location of the cysteine residue on the protein can be genetically engineered to address specific questions about intra- and interprotein electron transfer (9, 22–26, 36–39).

Extensive studies on a wide range of ruthenium-labeled proteins have provided important information on the dependence of electron transfer on driving force, distance, and pathway (7–39). The theory developed by Marcus has revealed that two important factors control the rate of electron transfer: the reorganization energy and the electronic coupling between the redox centers (40, 41). The reorganization energy λ is a measure of the energy required to rearrange and repolarize the reactants and surrounding solvent before electron transfer can occur. Dutton and co-workers have reported that the rate constants in a broad range of biological systems can be described approximately by a simple exponential dependence on the distance between the redox centers, as originally proposed by Marcus (42):

$$k_{\text{et}} = k_0 \exp[-\beta(r - r_0)] \exp[-(\Delta G^{\circ'} + \lambda)^2/4\lambda RT] \quad (1)$$

where r is the distance between the closest macrocycle atoms in the two redox centers, the van der Waals contact distance $r_0 = 3.6 \text{ \AA}$, $\beta = 1.4 \text{ \AA}^{-1}$, and the nuclear frequency $k_0 = 10^{13} \text{ s}^{-1}$. Beratan and Onuchic have developed a dominant pathway model in which the electronic coupling is described by a combination of covalent bond, hydrogen bond, and through-space contributions (43). More comprehensive discussions of electron-transfer theory are found in several recent reviews (44–46).

Two design criteria must be satisfied for the ruthenium photoexcitation technique to provide a reliable means of measuring intracomplex electron transfer. The ruthenium complex must not interfere with the conformation of the protein complex, and the rate of electron transfer from Ru(II*) to the first redox center must be fast compared to subsequent electron-transfer reactions under investigation. This requires an efficient pathway for electron transfer from Ru(II*) to the redox center, and optimum photoredox properties for Ru. A new yeast Ru-Cc derivative, Ru-39-Cc, was designed to satisfy both of these criteria for the reactions of Cc with its physiological electron-transfer partners (Figure 1). The single sulfhydryl at Cys-39 on the back surface of yeast H39C,C102T iso-1-Cc was labeled using method 4 to form Ru-39-Cc (9, 22). The binding constant and second-order rate constant for the reaction of Ru-39-Cc with both cytochrome oxidase (CcO) and cytochrome *c* peroxidase (CcP) are the same as for native yCc (9, 22). These results provide evidence that the ruthenium group on Ru-39-Cc does not affect the interaction with either CcO or CcP, an important criteria for the reliability of the method. The rate constant for electron transfer from Ru(II*) to the heme group is $5 \times 10^5 \text{ s}^{-1}$, consistent with good electronic coupling between the ruthenium complex and the heme group involving 13 covalent bonds and 1 hydrogen bond (Figure 1). The driving force of 1.1 eV is close to the reorganization energy of 0.74–1.0 eV, and thus the Franck–

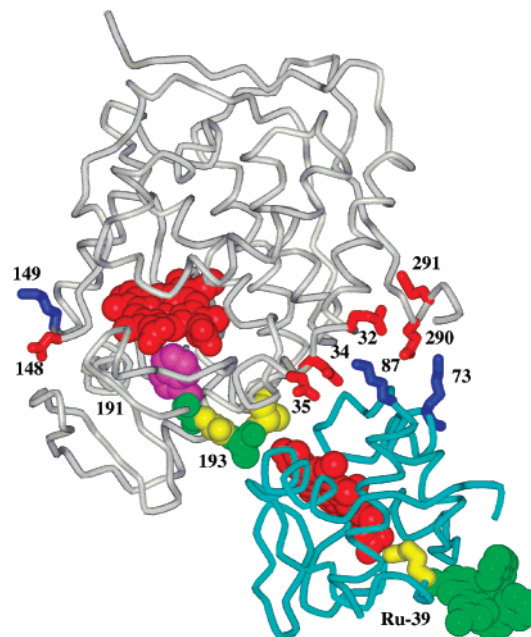
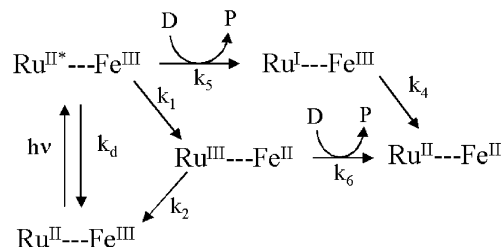


FIGURE 1: X-ray crystal structure of the CcP–yCc complex (52). The heme groups are shown in red CPK models, the Trp-191 indole group is purple, the Trp-191 backbone and Ala-193 are green, Gly-192 and Ala-194 are yellow, and Ru-39 is green. Cc residues 39–41 between Ru-39 and heme *c* are colored yellow. The side chains of CcP residues E32, D34, E35, E290, and E291, and yCc residues K73 and K87 are labeled. The low-affinity Cc binding site is proposed to be located near D148 and K149, which are labeled (71).

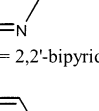
Scheme 2



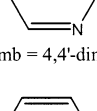
Condon term in eq 1 is close to the maximum value (9).

A wide range of different ruthenium complexes and sacrificial electron donors have been investigated to optimize both the rate and yield of photoreduction of heme iron using the reaction paths shown in Scheme 2. Heme Fe(III) can be reduced by Ru(II*) in steps k_1 and k_6 using a sacrificial donor (D) such as aniline. We have also found that a donor with a lower potential such as *N,N*-dimethylaminobenzoate can directly reduce Ru(II*) in step k_5 , followed by electron transfer from Ru(I) to heme Fe(III) in step k_4 (47). One of the advantages of the cysteine labeling chemistry is that all three chelating ligands can be varied to tune the redox properties of the ruthenium complex to optimize photochemical production of the desired products. The redox potentials of some of these complexes are shown in Table 1 (48). Ru-39-Cc and Ru-65-cyt b_5 derivatives with many of these complexes have been used to measure electron transfer as a function of driving force ΔG , spanning both the normal and the inverted Marcus region, to determine the reorganization energy λ (36–39). The bipyridazine ligand has been found to have significant promise for photoreduction studies. For example, Ru(bpd) $_2$ (dmb) has a large positive potential

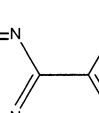
Table 1: Standard Reduction Potentials of Ruthenium Complexes vs NHE




bpy = 2,2'-bipyridine



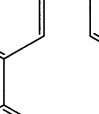
dmb = 4,4'-dimethyl-2,2'-bipyridine



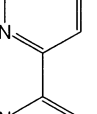
bpz = 2,2'-bipyrazine (1,4 N)



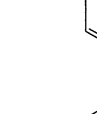
bpd = 3,3'-bipyridazine (1, 6 N)



bpm = 2,2'-bipyrimidine (1,3 N)



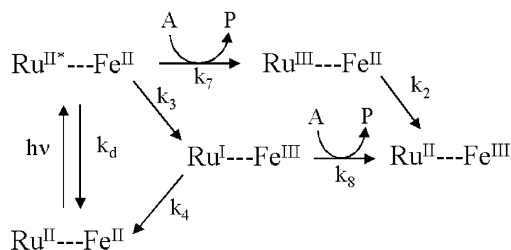
qpy = quaterpyridine



bphb

complex	(III)/(II)	(III)/(II*)	(II)/(I)	(II*)/(I)
Ru(bpy) ₃	1.27	−0.87	−1.31	0.83
Ru(bpy) ₂ (dmb)	1.27	−0.83	−1.36	0.79
Ru(dmb) ₃	1.17	−0.94	−1.44	0.67
Ru(bpz) ₂ (dmb)	1.76	−0.25	−0.79	1.22
Ru(bpd) ₂ (dmb)	1.49	−0.49	−1.00	0.98
Ru(bpm) ₂ (dmb)	1.55	−0.30	−0.95	0.90

Scheme 3



for the Ru(II*)/Ru(I) reaction, which provides efficient reduction of Ru(II*) to Ru(I) by *N,N*-dimethylaminobenzoate (Table 1). Subsequent electron transfer from Ru(I) to heme Fe(III) is also very favorable, giving a large k_4 . The Ru-39-Cc derivative with this complex has a yield of 35% for photoreduction of heme *c* with a single laser flash (49).

The ruthenium technique has also been used for photooxidation of heme iron according to Scheme 3. Rapid Scheme 4

photooxidation of reduced heme was observed in Ru-Cc derivatives in the presence of the sacrificial oxidant Co(NH₃)₅Br²⁺. Ru(II*) is oxidized to Ru(III) by Co(NH₃)₅Br²⁺, followed by oxidation of Fe(II) by Ru(III) with rate constant k_2 . The Ru(bpz)₂(dmb) complex is particularly effective for photooxidation. The driving force for the Ru(II*)-Fe(II) → Ru(I)-Fe(III) reaction (1.0 V) is close to the value of λ , leading to a large value of k_3 , $3.5 \times 10^6 \text{ s}^{-1}$. The resulting Ru(I) is rapidly oxidized by O₂ under aerobic conditions in step k_7 , leading to 20% photooxidation yield in a single flash (49).

Ruthenium complexes which interact noncovalently with proteins have been used for photochemical reduction or oxidation. Nilsson found that the positively charged complex Ru(bpy)₃²⁺ photochemically reduced Cu_A of CcO using Scheme 2 (50). The novel binuclear ruthenium complexes [Ru(bpy)₂]₂(bphb) and [Ru(bpy)₂]₂(qpy) were designed with a net charge of +4 which allow them to bind strongly to the acidic domain on subunit II of CcO and donate electrons specifically to Cu_A upon photolysis. The yield of reduced CcO obtained with a single laser flash is more than 5-fold larger than obtained with Ru(bpy)₃²⁺ (11). The complex [Ru(bpy)₂]₂(qpy) has also been found to photooxidize cyt *c*₁ in the cyt *bc*₁ complex with a yield of 25% using Scheme 3 (15). Recently, a new complex, [Ru(bpz)₂]₂(qpy), has been designed which photoreduces cyt *c*₁ in the cytochrome *bc*₁ complex with a yield of greater than 50% using Scheme 2 (S. Rajagukguk et al., manuscript in preparation). Gray and co-workers have recently designed a ruthenium-linked substrate in which Ru(bpy)₃ is linked by a hydrocarbon chain to adamantane, which has a high affinity for the cytochrome P450 binding pocket (51). This substrate could rapidly reduce or oxidize the heme group in cytochrome P-450 upon photooxidation of Ru(bpy)₃ in the presence of reductive or oxidative quenchers (51).

Cytochrome *c* Peroxidase (CcP). The reaction between Cc and CcP has become one of the most important prototypes for investigating fundamental questions about biological electron transfer. The reaction is initiated when hydrogen peroxide oxidizes the resting ferric state of CcP to CMPI (Fe^{IV}=O, R^{•+}), which contains an oxyferryl heme Fe^{IV}=O and an indolyl radical cation, R^{•+}, located on Trp-191 (52–60). CMPI is then sequentially reduced to CMPII and CcP by two molecules of Cc(II). An important question is whether Cc initially reduces the oxyferryl heme or the radical cation (61–63). The yeast Ru-Cc derivative, Ru-39-Cc, was specifically designed to measure the true rates of electron transfer to the radical cation and the oxyferryl heme in CMPI. Laser excitation of a 1:1 Ru-39-Cc/CMPI complex at low ionic strength resulted in rapid electron transfer from Ru(II*) to heme *c* Fe(III), followed by electron transfer from heme *c* Fe(II) to the Trp-191 radical cation in CMPI with rate constant $k_{\text{eta}} = 2.0 \times 10^6 \text{ s}^{-1}$ (Figure 1; Scheme 4) (22). A

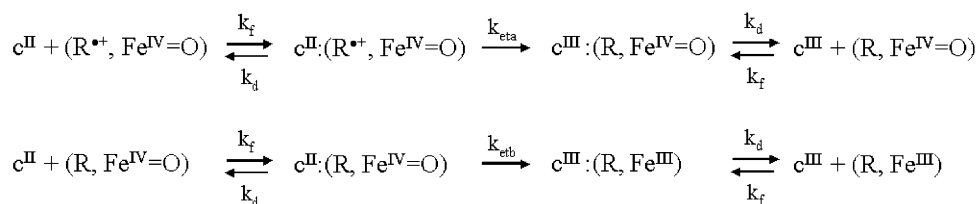


Table 2: Effect of CcP Mutants on Reaction with Ru-39-Cc^a

mutant	$k_{\text{eta}} \times 10^{-6} \text{ s}^{-1}$	$k_{\text{etb}} \times 10^{-3} \text{ s}^{-1}$	$K_d (\mu\text{M})$
CcP	2.0	5.0	0.6
E32Q	2.1	4.3	0.9
D34N	0.5	1.2	13
E35Q	0.8	2.3	1.2
E290N	0.9	2.0	11
E291Q	2.0	4.4	0.8
A193F	0.8	1.5	5.1

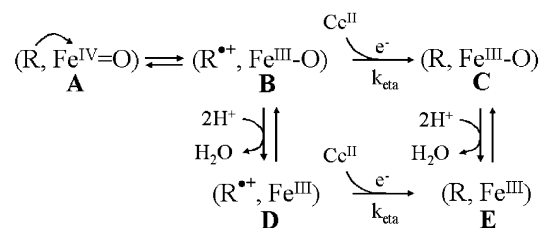
^a k_{eta} and k_{etb} were measured at 5 mM and K_d at 100 mM ionic strength (22, 23).

subsequent laser flash led to electron transfer from heme *c* Fe^{II} to the oxyferryl heme in CMPII($\text{Fe}^{\text{IV}}=\text{O}, \text{R}$) with rate constant $k_{\text{etb}} = 5000 \text{ s}^{-1}$. Ruthenium photoreduction studies with a wide range of horse and yeast Ru-Cc derivatives as well as stopped-flow studies with native hCc and yCc have demonstrated that the Trp-191 radical cation is the initial site of reduction in CMPI under all conditions of pH and ionic strength (16–24, 64).

Pelletier and Kraut (52) have determined the crystal structure of the complex between yeast iso-1-Cc (yCc) and CcP, and have proposed an electron-transfer pathway that extends from the exposed heme methyl group of Cc through CcP residues Ala-194, Ala-193, and Gly-192 to the indole group of Trp-191 (Figure 1). The effects of CcP surface mutations on K_d , k_{eta} , and k_{etb} provide strong evidence that the P–K crystalline binding domain is used for the reaction of Ru-39-Cc with both the radical cation and the oxyferryl heme in solution (22, 23) (Table 2, Figure 1). The mutations D34N, E290N, and A193F each decreased both k_{eta} and k_{etb} by 3–4-fold and increased the dissociation constant K_d of the complex between Ru-39-Cc and CMPI by 10–20-fold (Table 2). Asp-34 and Glu-290 interact electrostatically with yCc lysines 87 and 73, respectively, within the P–K binding domain (Figure 1). The Ala-193 methyl group is in van der Waals contact with the heme CBC methyl group at the center of the P–K binding domain. The value of k_{eta} was independent of viscosity and temperature, indicating that it is not controlled by conformational gating, but is the true rate constant for electron transfer from the Cc heme to the Trp-191 radical cation (24). This system, therefore, provides an excellent opportunity to compare the experimental rate constant with Marcus theory predictions based on the crystal structure. The distance between the closest heme macrocycle atom of yCc and the closest Trp-191 indole ring atom in CcP is 16.0 Å in the P–K crystal structure. It is assumed that the driving force $-\Delta G^\circ$ equals the reorganization energy λ , since k_{eta} is independent of temperature. Application of eq 1 with the parameters suggested by Dutton (42) gives a theoretical rate constant of $k_{\text{et}} = 3 \times 10^5 \text{ s}^{-1}$, which is in reasonable agreement with the experimental value of $k_{\text{eta}} = 2 \times 10^6 \text{ s}^{-1}$ (22). The best pathway between heme *c* and the Trp-191 indolyl radical cation consists of 11 covalent bonds and a van der Waals contact of 4.1 Å between the heme CBC methyl group and the Ala-193 methyl group.

Ruthenium photoreduction experiments have provided evidence that reduction of CMPII($\text{Fe}^{\text{IV}}=\text{O}, \text{R}$) involves rapid internal electron transfer leading to transient formation of the radical cation in CMPII($\text{Fe}^{\text{III}}, \text{R}^{\bullet+}$), which is then reduced by yCc^{II} in the high-affinity binding site (Scheme 5) (18, 20, 22). The steps $\text{A} \rightarrow \text{B} \rightarrow \text{D}$ in Scheme 5 have a rate

Scheme 5

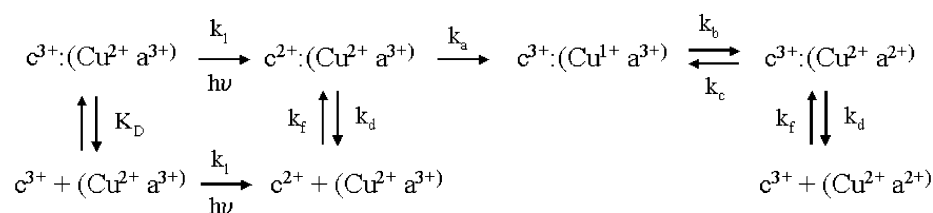


constant of 1100 s^{-1} (20), which is rate-limited by proton transfer to the oxygen atom on the iron. Reduction of CMPII($\text{Fe}^{\text{IV}}=\text{O}, \text{R}$) by low concentrations of solution Cc^{II} involves steps $\text{A} \rightarrow \text{B} \rightarrow \text{D} \rightarrow \text{E}$ with second-order rate constant k_b (22). It is proposed that reduction of oxyferryl heme by bound Cc^{II} involves the steps $\text{A} \rightarrow \text{B} \rightarrow \text{C} \rightarrow \text{E}$ with rate constant $k_{\text{etb}} = 5000 \text{ s}^{-1}$ (22). Proton transfer would be faster in the $\text{C} \rightarrow \text{E}$ step than in the $\text{B} \rightarrow \text{D}$ step due to electrostatic repulsion by the radical cation. The rate of reduction of the oxyferryl heme by yCc^{II} was decreased more than 10 000-fold by mutating Trp-191 to Phe, demonstrating the critical role of the Trp-191 radical cation (54). Thus, both steps in the complete reduction of CMPI involve electron transfer from Cc^{II} to the Trp-191 radical cation using the P–K binding site and pathway.

Kang et al. (65) and Kornblatt and English (66) have shown that a second molecule of Cc can bind to a low-affinity site on the 1:1 complex to form a 2:1 complex at low ionic strength. The binding of Cc to the low-affinity site increases the rate constant for reduction of the oxyferryl heme measured by both steady-state and stopped-flow kinetics at low ionic strength (61, 67, 68). Experiments using both the ruthenium photoreduction method and stopped-flow spectroscopy have indicated that yCc^{II} binding to the low-affinity site significantly increases the rate constant for dissociation of yCc^{III} from the high-affinity site in a substrate-assisted product dissociation mechanism (23, 69). Moreover, these techniques have provided evidence that the low-affinity Cc binding site is not significantly active in direct electron transfer to either the Trp-191 radical cation or the oxyferryl heme (23, 69). In contrast, Hoffman and co-workers have found that $^3\text{Zn-hCc}$ is active in electron transfer to the ferric heme from the low-affinity site on CcP, but is nearly inactive from the high-affinity site (70). However, the Trp-191 indole cannot be oxidized to the radical cation by the reductive ^3Zn porphyrin, and thus cannot be a redox intermediate in the reaction. The large separation between the $^3\text{Zn-hCc}$ in the high-affinity site and the CcP heme (26.5 Å metal-to-metal) would therefore limit the rate of electron transfer. Evidence has been presented that $^3\text{Zn-hCc}$ binds in the low-affinity site close to Asp-148 with a metal-to-metal distance of 22–25 Å (71), which would allow a faster rate of electron transfer than from the high-affinity site. Reduction of the CcP ferric heme by $^3\text{Zn-hCc}$ is a pure electron-transfer process, while reduction of the oxyferryl heme is a complex process involving proton transfer to the oxygen atom and release of water. Electron transfer from yCc to the oxyferryl heme is greatly accelerated by the use of the Trp-191 radical cation as a redox intermediate, and the presence of an efficient pathway from the high-affinity binding site.

The complete reduction of CMPI by two molecules of Cc^{II} requires at least two complex formation and dissociation steps

Scheme 6



and two intracomplex electron-transfer steps, as shown in Scheme 4. A ruthenium photoreduction technique was developed to measure the formation and dissociation rate constants k_f and k_d of the high-affinity complex between yeast iso-1-cytochrome *c* (yCc) and cytochrome *c* peroxidase compound I (CMPI) over a wide range of ionic strength (23). The value of k_d for the 1:1 high-affinity complex increases from $<5 \text{ s}^{-1}$ at low ionic strength to 4000 s^{-1} at 150 mM ionic strength, while k_f decreases from $>3 \times 10^9 \text{ M}^{-1} \text{ s}^{-1}$ at low ionic strength to $1.3 \times 10^9 \text{ M}^{-1} \text{ s}^{-1}$ at 150 mM ionic strength. The rate constants in Scheme 4 at physiological ionic strength (150 mM) are $k_f = 1.3 \times 10^9 \text{ M}^{-1} \text{ s}^{-1}$, $k_d = 4000 \text{ s}^{-1}$, $k_{eta} = 1.0 \times 10^6 \text{ s}^{-1}$, and $k_{etb} = 3000 \text{ s}^{-1}$ (23). The rate-limiting step in enzyme turnover is product dissociation below 150 mM ionic strength, and reduction of the oxyferryl heme at higher ionic strength. The interaction between yCc and CcP is optimized at physiological ionic strength to allow both rapid substrate complex formation and product complex dissociation.

Cytochrome *c* Oxidase (CcO). Cytochrome *c* oxidase, the terminal member of the mitochondrial electron-transport chain, is a redox-linked proton pump that transfers electrons from cytochrome *c* to molecular oxygen (72, 73). Three of the redox-active centers, heme *a*, heme *a*₃, and Cu_B, are located in subunit I, while Cu_A is located in subunit II. Cu_A consists of two copper atoms bridged by the sulfur atoms of Cys-196 and Cys-200. The characterization of the electron-transfer reaction from cytochrome *c* to the initial acceptor in cytochrome *c* oxidase has been a difficult problem. Flow-flash photolysis studies of the complex between ferrocyclochrome *c* and reduced-CO-inhibited cytochrome *c* oxidase indicated that heme *c* transferred an electron to Cu_A with a rate constant greater than $7 \times 10^4 \text{ s}^{-1}$ (74). The Ru-39-Cc derivative was designed to measure intracomplex electron transfer to the initial acceptor in CcO (9). Laser excitation of the 1:1 complex between Ru-39-Cc and beef CcO at low ionic strength leads to the electron-transfer sequence: $\text{Ru(II}^*) \rightarrow \text{heme } c^{3+} \rightarrow \text{Cu}_A^{2+} \rightarrow \text{heme } a^{3+}$ with rate constants of $k_1 = 5 \times 10^5 \text{ s}^{-1}$, $k_a = 6 \times 10^4 \text{ s}^{-1}$, and $k_b = 1.8 \times 10^4 \text{ s}^{-1}$, according to Scheme 6 (Figure 2) (9). As the ionic strength is increased from 40 to 100 mM, the amplitude of the fast phase decreases as the 1:1 complex dissociates, and a slow phase appears due to intermolecular reaction between free Ru-39-Cc and CcO. The intracomplex rate constant k_a does not change from low ionic strength up to over 100 mM ionic strength, indicating that the orientation of the complex does not change as a function of ionic strength. Both intracomplex and intermolecular phases were observed simultaneously in the ionic strength range 55–105 mM, which allowed the determination of complex formation and dissociation rate constants. At physiological ionic strength (100 mM), the complete reaction involves substrate complex formation between Cc^{2+} and CcO with rate constant $k_f = 1.8 \times 10^8$

$\text{M}^{-1} \text{ s}^{-1}$, intracomplex electron transfer from Cc^{2+} to Cu_A^{2+} with rate constant $k_a = 6 \times 10^4 \text{ s}^{-1}$, and product complex dissociation with rate constant $k_d = 8 \times 10^3 \text{ s}^{-1}$ (Scheme 6) (9).

A prominent cluster of acidic residues on subunit II near the binuclear Cu_A center is apparent in the X-ray crystal structures of bovine (75, 76) and *P. denitrificans* (77) CcO. Trp-143, a highly conserved aromatic residue at the center of this acidic cluster, is in van der Waals contact with the Cu_A center and could form an electron-transfer pathway from the surface of subunit II to Cu_A. The location of the binding domain for Cc on subunit II of CcO was investigated using a series of *R. sphaeroides* CcO mutants in which acidic residues were replaced with neutral Asn or Gln residues (Figure 3, Table 3) (10). In the 1:1 complex between Ru-55-Cc and wild-type CcO at low ionic strength, electron transfer from photoreduced heme *c* to Cu_A occurs with an intracomplex rate constant of $k_a = 4 \times 10^4 \text{ s}^{-1}$, followed by electron transfer from Cu_A to heme *a* with a rate constant of $k_b = 9 \times 10^4 \text{ s}^{-1}$. The D214N mutation decreased the intracomplex electron-transfer rate constant k_a to 700 s^{-1} , indicating a significant change in the binding orientation of Ru-55-Cc. The E157Q, E148Q, and D195N mutations also decreased the value of k_a by 2–4-fold. The D214N, E157Q, E148Q, and D195N mutations all significantly increase the

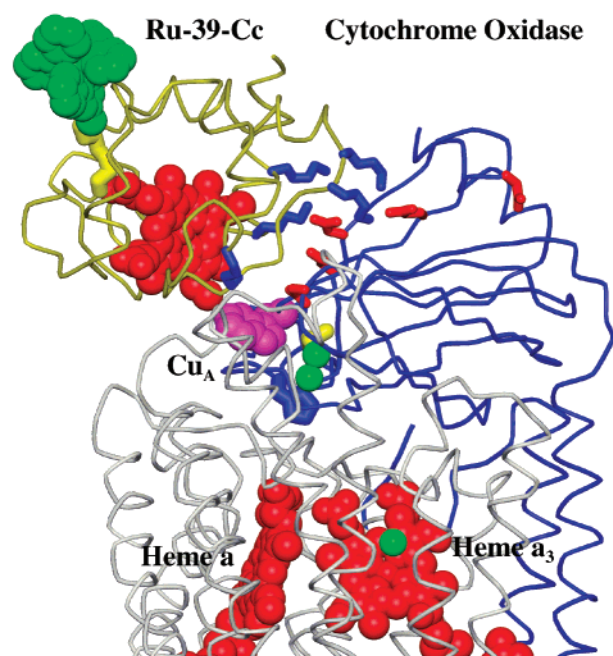


FIGURE 2: Complex between Ru-39-Cc and CcO. Ru-39-Cc is bound to CcO in the configuration determined by Roberts and Pique (84). The Cc backbone is colored yellow, CcO subunit I is gray, and CcO subunit II is blue. Subunit II Trp-143, Met-263, and His-260 are colored purple, yellow, and blue, respectively. Cc lysines 8, 13, 72, 86, and 87 are colored blue, while subunit II Glu-148, Asp-151, Glu-157, Asp-195, and Asp-214 are colored red.

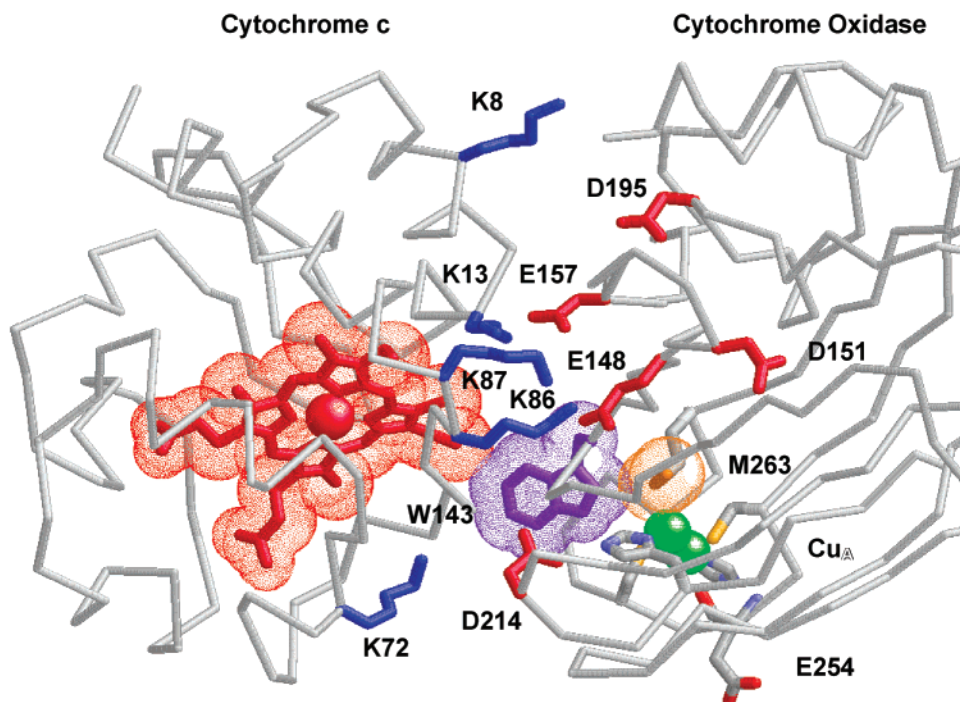


FIGURE 3: Model for the high-affinity complex between horse Cc and CcO determined by Roberts and Pique (84). The backbone of horse Cc and CcO subunit II are shown with the side chains of selected lysines and acidic residues colored blue and red, respectively. The residue numbers on subunit II are for *Rb. sphaeroides* CcO. van der Waals surfaces are shown for Cc heme, and subunit II Trp-143 and Met-263. The Cu_A coppers are represented by green CPK models.

Table 3: Reaction of Ru-55-Cc with *R. sphaeroides* Cytochrome Oxidase Mutants^a

CcO mutant	k_a (s ⁻¹)	K_d (μM)	k_{second} (μM ⁻¹ s ⁻¹)
wild-type	38000	1.0	310
W143A	32	0.9	0.6
W143F	85	1.5	1.7
E148Q	15000	2.3	125
D151N/D152Q	45000	1.6	192
E157Q	12000	3.9	58
D188N/E189Q	45000	1.3	285
D195N	25000	2.3	152
D214N	700	3.2	37
E254A	10500	1.0	120

^a The intracomplex rate constant k_a for electron transfer from heme *c* to Cu_A, the dissociation constant K_d , and the second-order rate constant k_{second} were at 5 mM, 45 mM, and 95 mM ionic strength, respectively, at pH 8 and 23 °C (10).

dissociation constant K_D , indicating that these mutations affect both binding strength and orientation. The D151N/E152Q and D188N/E189Q double mutants have essentially the same k_a , K_D , and k_{second} values as wild-type CcO, indicating that the mutated residues are outside the binding domain. The potential role of Trp-143 in mediating electron transfer from the heme group of Cc to Cu_A was investigated by substituting this residue with Phe or Ala. The intracomplex electron-transfer rate constant k_a was decreased 450-fold and 1200-fold by the mutations W143F and W143A, respectively (10). Since these mutations have no effect on binding strength, it is proposed that they cause a substantial disruption in the pathway for electron transfer rather than simply leading to a change in the orientation of the complex.

The kinetic studies of the surface mutants indicate that Cc binds to a highly conserved acidic domain on the surface of subunit II (Figures 2 and 3). The negatively charged carboxylates on residues Asp-214, Glu-157, Glu-148, and

Asp-195 interact with positively charged residues on Cc. Chemical modification studies have demonstrated that the positively charged amino groups on lysines 8, 13, 72, 86, and 87 surrounding the heme crevice of Cc are involved in the interaction with CcO (78–83). Roberts and Pique have used a computational program to propose a structure for the complex between Cc and CcO that is consistent with the kinetic studies (Figure 3)(84). The interaction consists of a central hydrophobic domain, surrounded by complementary electrostatic interactions between Cc lysines 8, 13, 86/87, 72, and CcO Asp-195, Glu-157, Glu-148, and Asp-214, respectively. The indole ring of Trp-143 is in van der Waals contact with the heme CBC methyl group at the center of the hydrophobic domain. The closest distance between the heme *c* macrocycle and the Met-263 Cu_A ligand is 12.5 Å in the Cc/CcO model complex. Using this distance, a theoretical electron-transfer rate constant of 6×10^4 s⁻¹ is calculated from the Marcus eq 1, assuming $\lambda = 0.65$ eV and $\Delta G^\circ = -0.03$ eV. This is in good agreement with the experimental values of $k_{\text{et}} = 6 \times 10^4$ s⁻¹ for the reaction between Ru-39-Cc and Cu_A in beef CcO (9), and 4×10^4 s⁻¹ for the reaction between Ru-55-Cc and Cu_A in *R. sphaeroides* CcO (10). Electronic coupling is extremely good because the indole ring of Trp-143 is in direct van der Waals contact with both the Cc heme and the Cu_A ligands Cys-256 and Met-263 (Figure 3).

The Cu_A center in CcO has a novel binuclear structure in which the two copper atoms are bridged by the sulfur atoms of Cys-252 and Cys-256. His-217 and Met-263 are terminal ligands to one copper atom, and His-260 and the backbone carbonyl of Glu-254 are terminal ligands to the other copper atom (*R. sphaeroides* CcO sequence numbering). To investigate the mechanism of electron transfer from Cc to Cu_A and heme *a*, two *R. sphaeroides* CcO mutants were exam-

ined, M263L and H260N (85). Met-263 ligates the copper that is closest to Cc, while His-260 ligates the copper that is linked by a hydrogen-bond network to heme *a*. In both of these mutants, two copper atoms are retained at the Cu_A center, but the redox potential of Cu_A was increased by 120 mV for the M263L mutant and by 90 mV for the H260N mutant. The mixed-valence Cu(1.5)••Cu(1.5) state of the wild-type Cu_A center appears to be converted to a state in which the two copper atoms are no longer equivalent. The rate constant for intracomplex electron transfer from heme *c* to Cu_A is 16 000 s⁻¹ for M263L CcO and 11 000 s⁻¹ for H260N CcO, compared to 40 000 s⁻¹ for wild-type CcO. The rate constants for electron transfer between Cu_A to heme *a* are $k_b = 4000 \text{ s}^{-1}$ and $k_c = 66\,000 \text{ s}^{-1}$ for M263L CcO and $k_b = 45 \text{ s}^{-1}$ and $k_c = 180 \text{ s}^{-1}$ for H260N, compared to $k_b = 90\,000 \text{ s}^{-1}$ and $k_c = 17\,000 \text{ s}^{-1}$ for wild-type CcO. The effects of the M263L mutation on the kinetics appear to be largely due to the increase in redox potential of the Cu_A center. However, the large decrease in the rate constants for electron transfer between Cu_A and heme *a* in the H260N mutant is due to a disruption in the structure between the two centers. It has been proposed that the pathway for electron transfer from Cu_A to heme *a* involves a hydrogen-bond network through the Cu_A ligand His-260, the peptide backbone, and the highly conserved subunit I residue Arg-482 to the heme *a* propionates (75–77, 86, 87). The large decrease in the rate constants for electron transfer between Cu_A and heme *a* in the H260N mutant provides experimental evidence for the involvement of this pathway in electron transfer.

The reduction of oxygen by CcO involves binding O₂ to the reduced heme *a*₃–Cu_B binuclear center and two-electron reduction to form the peroxy (P) state followed by successive one-electron reduction steps to the oxyferryl (F) state and the resting oxidized (O) state (72, 73). Wikstrom has shown that proton pumping is coupled to reduction of the P and F states (73). Compound F, which contains an oxyferryl heme *a*₃ (Fe⁴⁺=O²⁻), can be obtained by treatment with hydrogen peroxide (88). Electron transfer within compound F has been studied by injecting an electron into Cu_A by photolysis of either Ru(bpy)₃²⁺ (50) or [Ru(bpy)₂]₂(bphb), which has a net charge of +4 and binds strongly to subunit II of CcO near Cu_A (11). Following electron transfer from photoexcited [Ru(bpy)₂]₂(bphb)* to Cu_A within less than 1 μs, Cu_A transfers an electron to heme *a* with a rate constant of $2.0 \times 10^4 \text{ s}^{-1}$. Reduced heme *a* then transfers an electron to oxyferryl heme *a*₃ in compound F with a rate constant of $k_d = 470 \text{ s}^{-1}$. Reduction of the oxyferryl heme *a*₃, monitored at 580 nm, occurs simultaneously with oxidation of heme *a* monitored at 605 nm, indicating that an intermediate with an electron on Cu_B does not transiently accumulate (11). Experiments in D₂O revealed a deuterium kinetic isotope effect of 4.3, indicating that electron transfer from heme *a* to oxyferryl heme *a*₃ is rate-limited by a proton-transfer step, ultimately leading to protonation of the oxygen atom on the oxyferryl heme *a*₃ iron and formation of Fe³⁺–OH⁻. Konstantinov and co-workers have developed an electrometric method to measure the kinetics of electrogenic proton translocation in CcO following electron injection from photoexcited Ru(bpy)₃²⁺ (89). It was found that two protons were translocated across the membrane in both the P → F and F → O electron-transfer steps (89). Mutations in the K channel (K362M) had

no effect on the F → O transition, while mutations in the D channel (D132N) strongly inhibited electrogenic proton transfer in the F → O step (90). These results suggest that the D channel is involved in uptake of both “chemical” and “pumped” protons, while the K channel is used for loading the enzyme with protons at an earlier step in the catalytic cycle. Ruthenium photoreduction techniques continue to provide important information on the mechanism of electron transfer and proton translocation in CcO.

Cytochrome *bc*₁ Complex. Cytochrome *bc*₁ is perhaps the most universal electron-transfer complex, and is found in eukaryotic mitochondria as well as many prokaryotes (91). The complex contains two *b* cytochromes, *b*_L and *b*_H, located in a single polypeptide, the Rieske iron–sulfur protein, and cytochrome *c*₁ (91, 92). In the generally accepted Q cycle mechanism, four protons are translocated to the positive (P) side of the membrane per two electrons transferred from ubiquinol to Cc (91–93). A key bifurcated reaction takes place at the Q_o site, in which the first electron is transferred from ubiquinol to the Rieske iron–sulfur center (2Fe2S), and then to cyt *c*₁ and cyt *c* (91–93). The resulting semiquinone in the Q_o site transfers the second electron to cyt *b*_L and then to cyt *b*_H and ubiquinone in the Q_i site. X-ray crystallographic studies of cyt *bc*₁ have shown that the Rieske iron–sulfur protein assumes different conformations in different crystal forms and in the presence of Q_o site inhibitors (Figure 4) (94–98). The Rieske iron–sulfur protein is in a conformation with 2Fe2S proximal to the cyt *b*_L heme, called the *b* state, in bovine, chicken, and yeast cyt *bc*₁ crystals grown in the presence of stigmatellin, (95, 96, 98). In contrast, the Rieske iron–sulfur protein is in a conformation with 2Fe2S close to cyt *c*₁, called the *c*₁ state, in native chicken or bovine P6₅22 crystals (Figure 4) (95, 96). In native I₁22 bovine crystals, a major portion of the Rieske iron–sulfur protein appears to be conformationally mobile (94, 97). A novel shuttle mechanism for the Rieske iron–sulfur protein has been suggested on the basis of these structural studies. The Rieske protein is proposed to change conformation from the *b* state, where oxidized 2Fe2S accepts an electron from ubiquinol in the Q_o site, to the *c*₁ state, where reduced 2Fe2S transfers an electron to cyt *c*₁ (94–97).

To understand the mobile shuttle mechanism, it is important to determine the dynamics of conformational changes in the Rieske iron–sulfur protein, and the rate constants for electron transfer from quinol to 2Fe2S, and from 2Fe2S to cyt *c*₁. However, only limited kinetic information was previously available on the intracomplex electron-transfer reactions involving the Rieske center, cyt *c*₁, and Cc. Previous experiments in chromatophores from *R. sphaeroides* were limited by the rate of diffusion of photooxidized cyt *c*₂ from the reaction center to the *bc*₁ complex, which has a rate constant of about 5000 s⁻¹ (99). A lower limit for intracomplex electron transfer between the Rieske center and cyt *c*₁ was estimated to be 10⁵ s⁻¹ using this technique (99). A new method has been developed to study electron transfer within the cyt *bc*₁ complex using the binuclear ruthenium complex [Ru(bpy)₂]₂(qpy) (Scheme 7) (15). The 4+ charge on [Ru(bpy)₂]₂(qpy) allows it to bind with high affinity to the negatively charged binding domain on the surface of cyt *c*₁ as a surrogate for Cc. Photoexcitation of [Ru(bpy)₂]₂(qpy) to the metal-to-ligand charge-transfer state, [Ru(bpy)₂]₂(qpy)*, results in reduction or oxidation of cyt *c*₁ within 1

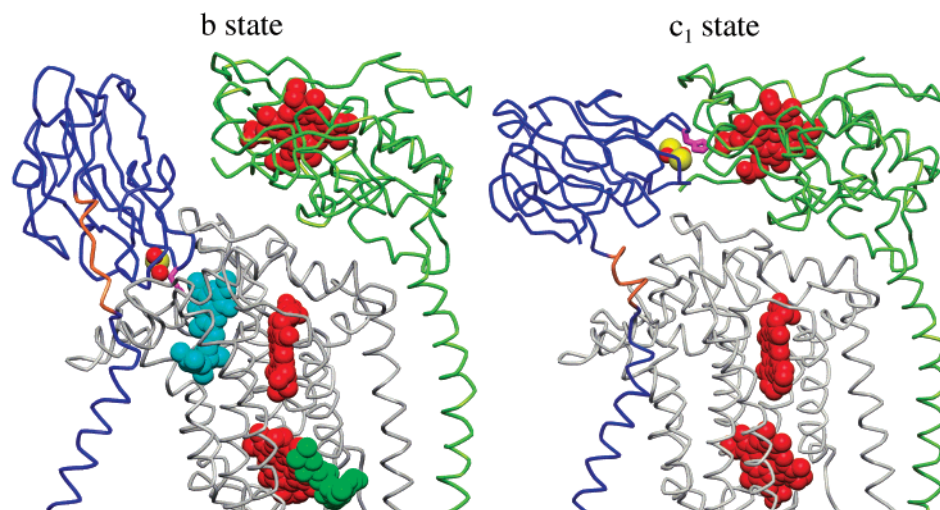
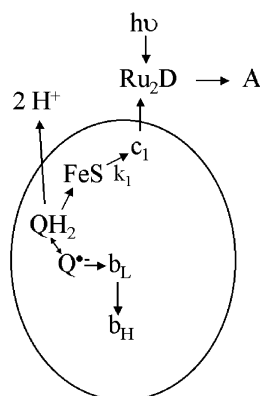


FIGURE 4: X-ray crystal structures of cytochrome *bc*₁ from chicken in the presence of stigmatellin and antimycin (*b* state) (95), and in the beef *P6522* crystals (*c*₁ state) (96). The Rieske, cyt *c*₁, and cyt *b* subunits are colored blue, green, and gray, respectively. The hemes, the 2Fe2S center, stigmatellin, and antimycin are represented by CPK models colored red, red/yellow, cyan, and green, respectively. The Rieske neck region residues 66–72 are colored orange, and His-161 is colored purple.

Scheme 7



μ s in the presence of appropriate sacrificial reductants or oxidants. Reduced cyt *c*₁ is photooxidized by [Ru(bpy)₂]₂-(qpy) in the presence of the sacrificial electron acceptor [Co(NH₃)₅Cl]²⁺ as shown in Scheme 3.

Electron transfer in the *R. sphaeroides* cyt *bc*₁ complex has been studied using [Ru(bpy)₂]₂-(qpy) to photoinitiate the reaction (15). The reduction of photooxidized cyt *c*₁ has a fast phase with a rate constant of 80 000 s⁻¹ due to electron transfer from 2Fe2S to cyt *c*₁, and a slow phase with a rate constant of 1000 s⁻¹ due to rate-limiting electron transfer from QH₂ to 2Fe2S and cyt *c*₁, followed by rapid electron transfer from the semiquinone to cyt *b*_L and cyt *b*_H (Scheme 7). A series of experiments were carried out to determine whether the fast phase of electron transfer from 2Fe2S to cyt *c*₁ was rate-limited by pure electron transfer, proton gating, or conformational gating. The temperature dependence of the reaction yielded an enthalpy of activation of +17.6 kJ/mol, which is consistent with a mechanism involving rate-limiting conformational gating (100). However, the temperature dependence is also consistent with the Marcus theory of electron transfer (eq 1) with a distance of 11.3 Å between 2Fe2S and cyt *c*₁, and a reorganization energy of 1 eV. The rate constant was independent of pH even though the redox potential of 2Fe2S decreases significantly due to deprotonation of His-161. The reaction is, therefore, not rate-limited by proton gating. The rate constant

was also not changed by the Rieske protein mutations Y156W, S154A, or Y156F/S154A which decrease the redox potential of 2Fe2S by 62, 109, and 159 mV, respectively (100). The reaction is thus not rate-limited by electron transfer, since Marcus theory predicts that the increase in the driving force of the reaction for these mutants would increase the rate constant by up to 15-fold.

The effects of temperature, pH, and driving force indicate that the electron-transfer reaction from the Rieske iron–sulfur center to cyt *c*₁ is not rate-limited by true electron transfer, but rather by dynamic fluctuation in the conformation of the Rieske protein. This conformational gating mechanism requires that the fluctuations are slow compared to electron transfer in the active *c*₁ state and the population of the *c*₁ state is small. The rate constant for electron transfer in the active *c*₁ state must be much larger than the observed rate constant. The active *c*₁ state could be similar to the bovine *P6522* crystal structure (96), in which the iron–sulfur ligand His-161 forms a hydrogen bond with the heme *c*₁ propionate oxygen (Figure 4). This provides a direct pathway for electron transfer from the 2Fe2S center to the heme *c*₁ macrocycle with a distance of 7.8 Å from the His-161 nitrogen to the heme *c*₁ macrocycle atom C3D (Figure 4). The rate constant calculated from the Marcus eq 1 ranges from 1.5 × 10⁶ to 3 × 10⁷ s⁻¹ assuming λ values between 1.0 and 0.7 eV. The true rate of electron transfer in the active *c*₁ state could thus be considerably faster than the observed value of 8 × 10⁴ s⁻¹, satisfying the requirements of the conformational gating mechanism. The conformational fluctuations which gate the observed rate of electron transfer could involve the whole range of conformations from the *b* state to the *c*₁ state, or a smaller ensemble of conformations including the active *c*₁ state and intermediate states.

The conformational changes in the Rieske protein are localized in the “neck” region (residues 66–72), which is helical in the *c*₁ state and extended in the *b* state (Figure 4). The importance of conformational flexibility in this neck region has been evaluated using a double proline mutant which should increase the rigidity of the neck (15). This mutation decreases the rate of electron transfer between the iron–sulfur center and cyt *c*₁ from 80 000 to 25 s⁻¹,

demonstrating the critical role that the Rieske neck region plays in the conformational change between the *b* state and the *c*₁ state.

The electron-transfer reaction between Cc and bovine cytochrome *bc*₁ was studied using the ruthenium photo-reduction technique. Horse Ru-72-Cc was chosen because it has a high efficiency of photoreduction in a single flash (35%), allowing measurement of the rate constant for intracomplex electron transfer from heme *c* to cyt *c*₁ to be 60 000 s⁻¹ (14). However, the ruthenium complex on lysine 72 at the edge of the Cc heme crevice does appear to alter the binding strength and orientation of the complex with cyt *bc*₁, raising the question of how well the measured rate constant reflects the true rate constant in the native complex (14). Studies using a series of *Rhodobacter sphaeroides* cyt *bc*₁ mutants indicate that acidic residues on the intramembrane surface of cyt *c*₁ are involved in directing the diffusion and binding of Cc from the intramembrane space (14). A recent X-ray crystal structure revealed that the complex between yCc and yeast cytochrome *bc*₁ is stabilized by interactions between nonpolar residues, including a planar stacking interaction between yCc Arg-13 and Phe-230 of cyt *c*₁ (101). The distance between the edges of the heme *c* and heme *c*₁ groups is only 9.4 Å, leading to an estimated rate constant for electron transfer of between 8.3×10^6 and 9.7×10^5 s⁻¹ using eq 1 and assuming λ between 0.7 and 1.0 eV (101). Experiments are underway to measure this rate constant experimentally using a yeast Ru-39-Cc derivative labeled with the Ru(bpz)₂(dmb) complex, which is particularly effective for photooxidation. The ruthenium complex at Cys-39 on the back of Ru-39-Cc does not affect the binding interaction with cytochrome *bc*₁, indicating that this derivative should provide a reliable estimate of electron transfer in the native complex.

REFERENCES

- McLendon, G., and Miller, J. R. (1985) *J. Am. Chem. Soc.* 107, 7811–7816.
- Faher, G., Allen, J. P., Okamura, M. Y., and Rees, D. C. (1989) *Nature* 339, 111–116.
- Everest, A. M., Wallin, S. A., Stemp, E. D. A., Nocek, J. M., Mauk, A. G., and Hoffman, B. M. (1991) *J. Am. Chem. Soc.* 113, 4337–4338.
- Hazzard, J. T., Poulos, T. L., and Tollin, G. (1987) *Biochemistry* 26, 2836–2848.
- Szundi, I., Cappuccio, J. A., Borovok, N., Kotlyar, A. B., and Einarsson, O. (2001) *Biochemistry* 40, 2186–2193.
- Hill, B. C. (1991) *J. Biol. Chem.* 266, 2219–2226.
- Durham, B., Pan, L. P., Hall, J., and Millett, F. (1989) *Biochemistry* 28, 8659–8665.
- Pan, L. P., Hibdon, S., Liu, R.-Q., Durham, B., and Millett, F. (1993) *Biochemistry* 32, 8492–8498.
- Geren, L. M., Beasley, J. R., Fine, B. R., Saunders, A. J., Hibdon, S., Pielak, G. J., Durham, B., and Millett, F. (1995) *J. Biol. Chem.* 270, 2466–2472.
- Wang, K., Zhen, Y., Sadosky, R., Grinnell, S., Geren, L., Ferguson-Miller, S., Durham, B., and Millett, F. (1999) *J. Biol. Chem.* 274, 38042–38050.
- Zaslavsky, D., Sadoski, R. C., Wang, K., Durham, B., Gennis, R. B., and Millett, F. (1998) *Biochemistry* 37, 14910–14916.
- Wang, K., Geren, L., Zhen, Y., Ma, L., Ferguson-Miller, S., Durham, B., and Millett, F. (2002) *Biochemistry* 41, 2298–2304.
- Heacock, C., Liu, R., Yu, C.-A., Yu, L., Durham, B., and Millett, F. (1993) *J. Biol. Chem.* 268, 27171–27175.
- Tian, H., Sadoski, R., Zhang, L., Yu, C.-A., Yu, L., Durham, B., and Millett, F. (2000) *J. Biol. Chem.* 275, 9587–9595.
- Sadoski, R. C., Engstrom, G., Tian, H., Zhang, L., Yu, C.-A., Yu, L., Durham, B., and Millett, F. (2000) *Biochemistry* 39, 4231–4236.
- Geren, L. M., Hahm, S., Durham, B., and Millett, F. (1991) *Biochemistry* 30, 9450–9457.
- Hahm, S., Durham, B., and Millett, F. (1992) *Biochemistry* 31, 3472–3477.
- Hahm, S., Miller, M. A., Geren, L., Kraut, J., Durham, B., and Millett, F. (1994) *Biochemistry* 33, 1473–1480.
- Miller, M. A., Liu, R.-Q., Hahm, S., Geren, L., Hibdon, S., Kraut, J., Durham, B., and Millett, F. (1994) *Biochemistry* 33, 8686–8693.
- Liu, R.-Q., Hahm, S., Miller, M. A., Han, G. W., Geren, L., Hibdon, S., Kraut, J., Durham, B., and Millett, F. (1994) *Biochemistry* 33, 8678–8685.
- Liu, R., Hahm, S., Miller, M., Durham, B., and Millett, F. (1995) *Biochemistry* 34, 973–983.
- Wang, K., Mei, H., Geren, L., Miller, M. A., Saunders, A., Wang, X., Waldner, J. L., Pielak, G. J., Durham, B., and Millett, F. (1996) *Biochemistry* 35, 15107–15119.
- Mei, H., Wang, K., McKee, S., Wang, X., Waldner, J. L., Pielak, G. J., Durham, B., and Millett, F. (1996) *Biochemistry* 35, 15800–15806.
- Mei, H., Wang, K., Pfeffer, N., Weatherly, G., Cohen, D. S., Miller, M., Pielak, G., Durham, B., and Millett, F. (1999) *Biochemistry* 38, 6846–6854.
- Willie, A., Stayton, P. S., Sligar, S. G., Durham, B., and Millett, F. (1992) *Biochemistry* 31, 7237–7243.
- Willie, A., McLean, M., Liu, R. Q., Hilgen-Willis, S., Saunders, A. J., Pielak, G. J., Sligar, S. G., Durham, B., and Millett, F. (1993) *Biochemistry* 32, 7519.
- Winkler, J. R., Nocera, D. G., Yocom, K. M., Bordignon, E., and Gray, H. B. (1982) *J. Am. Chem. Soc.* 104, 5798–5800.
- Isied, S. S., Worosila, G., and Atherton, S. J. (1982) *J. Am. Chem. Soc.* 104, 7659–7661.
- Pan, L. P., Durham, B., Wolinska, J., and Millett, F. (1988) *Biochemistry* 27, 7180–7184.
- Liu, R.-Q., Geren, L., Anderson, P., Fairris, J. L., Pfeffer, N., McKee, A., Durham, B., and Millett, F. (1995) *Biochimie* 77, 549–561.
- Durham, B., Pan, L. P., Hahm, S., Long, J., and Millett, F. (1990) *Electron Transfer in Biology and the Solid State*. ACS Adv. Chem. Ser. 226, 181.
- Millett, F., and Durham, B. (1991) *Met. Ions Biol. Syst.* 27, 223–264.
- Wuttke, D. S., Bjerrum, M. J., Winkler, J. R., and Gray, H. B. (1992) *Science* 256, 1007–1009.
- Di Bilio, A. J., Dennison, C., Gray, H. B., Ramirez, B. E., Sykes, A. G., and Winkler, J. R. (1998) *J. Am. Chem. Soc.* 120, 7551–7556.
- Bjerrum, M. J., Casimiro, D. R., Chang, I., De Bilio, A. J., Gray, H. B., Hill, M. G., Langen, R., Mines, G. A., Skov, L. K., Winkler, J. R., and Wuttke, D. S. (1995) *J. Bioenerg. Biomembr.* 27, 295–302.
- Scott, J. R., Willie, A., McLean, M., Stayton, P. S., Sligar, S. G., Durham, B., and Millett, F. (1993) *J. Am. Chem. Soc.* 115, 6820.
- Scott, J. R., McLean, M., Sligar, S. G., Durham, B., and Millett, F. (1994) *J. Am. Chem. Soc.* 116, 7356–7362.
- Scott, J. R., Fairris, J. L., McLean, M., Wang, K., Sligar, S. G., Durham, B., and Millett, F. (1996) *Inorg. Chim. Acta* 243, 193.
- Fairris, J. L., Wang, K., Geren, L., Pielak, G. J., Durham, B., and Millett, F. (1998) *ACS Adv. Chem. Ser.* 254, 99–110.
- Marcus, R. A. (1956) *J. Chem. Phys.* 24, 966–989.
- Marcus, R. A., and Sutin, N. (1985) *Biochim. Biophys. Acta* 811, 265–322.
- Moser, C. C., Keske, J. M., Warncke, K., Farid, R. S., and Dutton, P. L. (1992) *Nature* 355, 796–802.
- Beratan, D. N., Betts, J. N., and Onuchic, J. N. (1992) *J. Chem. Phys.* 96, 2852–2855.
- Page, C. C., Moser, C. C., Chen, X., and Dutton, P. L. (1999) *Nature* 402, 47–52.
- Gray, H. B., and Winkler, J. R. (1966) *Annu. Rev. Biochem.* 65, 537–561.
- Davidson, V. L. (2000) *Acc. Chem. Res.* 33, 87–93.
- Heacock, D. H., II, Harris, M. R., Millett, F., and Durham, B. (1994) *Inorg. Chim. Acta* 226, 129.
- Rillema, D. P., Allen, G., Meyer, T. J., and Conrad, D. (1983) *Inorg. Chem.* 22, 1617–1622.

49. Rajagukguk, R., Patel, C., Pielak, G., Geren, L., Millett, F., and Durham, B. (2002) *Biophys. J.* 82, 286a.
50. Nilsson, T. (1992) *Proc. Natl. Acad. Sci. U.S.A.* 89, 6497–6501.
51. Wilker, J. J., Dmochowski, I. J., Dawson, J. H., Winkler, J. R., and Gray, H. B. (1999) *Angew. Chem., Int. Ed. Engl.* 38, 90–92.
52. Pelletier, H., and Kraut, J. (1992) *Science* 258, 1748–1755.
53. Millett, F., Miller, M. A., Geren, L., and Durham, B. (1995) *J. Bioenerg. Biomembr.* 27, 341–351.
54. Mauro, J. M., Fishel, L. A., Hazzard, J. T., Meyer, T. E., Tollin, G., Cusanovich, M. A., and Kraut, J. (1988) *Biochemistry* 27, 6243–6256.
55. Scholes, C. P., Liu, Y., Fishel, L. A., Farnum, M. F., Mauro, J. M., and Kraut, J. (1989) *Isr. J. Chem.* 29, 85–92.
56. Erman, J. E., Vitello, L. B., Mauro, J. M., and Kraut, J. (1989) *Biochemistry* 28, 7992–7995.
57. Sivaraja, M., Goodin, D. B., Smith, M., and Hoffman, B. M. (1989) *Science* 245, 738–740.
58. Miller, M. A., Han, G. W., and Kraut, J. (1994) *Proc. Natl. Acad. Sci. U.S.A.* 91, 11118–11122.
59. Fitzgrald, M. M., Churchill, M. J., McRee, D. E., and Goodin, D. B. (1994) *Biochemistry* 33, 3807–3818.
60. Huyett, J. E., Doan, P. E., Gurbiel, R., Houseman, A. L. P., Sivaraja, M., Goodin, D. B., and Hoffman, B. M. (1995) *J. Am. Chem. Soc.* 117, 9033–9041.
61. Matthis, A. L., Vitello, L. B., and Erman, J. E. (1995) *Biochemistry* 34, 9991–9999.
62. Nuevo, M. R., Chu, H.-H., Vitello, L. B., and Erman, J. E. (1993) *J. Am. Chem. Soc.* 115, 5873–5874.
63. Summers, F. E., and Erman, J. E. (1988) *J. Biol. Chem.* 263, 14267–14275.
64. Hahm, S., Geren, L., Durham, B., and Millett, F. (1993) *J. Am. Chem. Soc.* 115, 3372–3373.
65. Kang, C. H., Ferguson-Miller, S., and Margoliash, E. (1977) *J. Biol. Chem.* 252, 919–926.
66. Kornblatt, J. A., and English, A. M. (1986) *Eur. J. Biochem.* 155, 505–511.
67. Miller, M. A. (1996) *Biochemistry* 35, 15791–15799.
68. Matthis, A. L., and Erman, J. E. (1995) *Biochemistry* 34, 9985–9990.
69. Mei, H., Geren, L., Miller, M. A., Durham, B., and Millett, F. (2002) *Biochemistry* 41, 3968–3976.
70. Zhou, J. S., and Hoffman, B. M. (1994) *Science* 265, 1693–1696.
71. Leesch, V. W., Bujons, J., Mauk, A. G., and Hoffman, B. M. (2000) *Biochemistry* 39, 10132–10139.
72. Ferguson-Miller, S., and Babcock, G. T. (1996) *Chem. Rev.* 96, 2889–2907.
73. Babcock, G. T., and Wikstrom, M. (1992) *Nature* 356, 301–309.
74. Hill, B. C. (1991) *J. Biol. Chem.* 266, 2219–2226.
75. Tsukihara, T., Aoyama, H., Yamashita, E., Tomizaki, T., Yamaguchi, H., Shinzawa-Itoh, K., Nakashima, R., Yaono, R., and Yoshikawa, S. (1995) *Science* 269, 1069–1074.
76. Tsukihara, T., Aoyama, H., Yamashita, E., Tomizaki, T., Yamaguchi, H., Shinzawa-Itoh, K., Nakashima, R., Yaono, R., and Yoshikawa, S. (1996) *Science* 272, 1136–1144.
77. Iwata, S., Ostermeier, C., Ludwig, B., and Michel, H. (1995) *Nature* 376, 660–669.
78. Smith, H. T., Staudenmeyer, N., and Millett, F. (1977) *Biochemistry* 16, 4971–4977.
79. Staudenmeyer, N., Smith, M. B., Ng, S., and Millett, F. (1977) *Biochemistry* 16, 600.
80. Ferguson-Miller, S., Brautigan, D. L., and Margoliash, E. (1978) *J. Biol. Chem.* 253, 149–159.
81. Rieder, R., and Bosshard, H. R. (1980) *J. Biol. Chem.* 255, 4732–4741.
82. Osheroff, N., Brautigan, D. L., and Margoliash, E. (1980) *J. Biol. Chem.* 255, 8245–8251.
83. Smith, M. B., Stonehuerner, J., Ahmed, A. J., Staudenmeyer, N., and Millett, F. (1980) *Biochim. Biophys. Acta* 592, 303.
84. Roberts, V. A., and Pique, M. E. (1999) *J. Biol. Chem.* 274, 38051–38060.
85. Wang, K., Geren, L., Zhen, Y., Ma, L., Ferguson-Miller, S., Durham, B., and Millett, F. (2002) *Biochemistry* 41, 2298–2304.
86. Gamelin, D. R., Randall, D. W., Hay, M. T., Houser, R. P., Mulder, T. C., Canters, G. W., de Vries, S., Tolman, W. B., Lu, Y., and Solomon, E. I. (1998) *J. Am. Chem. Soc.* 120, 5246.
87. Regan, J. J., Ramirez, B. E., Winkler, J. R., Gray, H. B., and Malmstrom, B. G. (1998) *J. Bioenerg. Biomembr.* 30, 35.
88. Fabian, M., and Palmer, G. (1995) *Biochemistry* 34, 13802–13810.
89. Zaslavsky, D., Kaulen, A. D., Smirnova, I. A., Vygodina, T., and Konstantinov, A. A. (1993) *FEBS Lett.* 336, 389–393.
90. Konstantinov, A. A., Siletsky, S., Mitchell, D., Kaulen, A., and Gennis, R. B. (1997) *Proc. Natl. Acad. Sci. U.S.A.* 94, 9085–9090.
91. Trumpower, B. L., and Gennis, R. B. (1994) *Annu. Rev. Biochem.* 63, 675–716.
92. Trumpower, B. L. (1990) *J. Biol. Chem.* 265, 11409–11412.
93. Brandt, U. (1998) *Biochim. Biophys. Acta* 1364, 261–268.
94. Xia, D., Yu, C.-A., Kim, H., Xia, J.-Z., Kachurin, A. M., Zhang, L., Yu, L., and Deisenhofer, J. (1997) *Science* 277, 60–66.
95. Zhang, Z., Huang, L., Shulmeister, V. M., Chi, Y.-I., Kim, K. K., Hung, L.-W., Crofts, A. R., Berry, E. A., and Kim, S.-H. (1998) *Nature* 392, 677–684.
96. Iwata, S., Lee, J. W., Okada, K., Lee, J. K., Wata, M., Rasmussen, B., Link, T. A., Ramaswamy, S., and Jap, B. K. (1998) *Science* 281, 64–71.
97. Kim, H., Xia, D., Yu, C.-A., Xia, J.-Z., Kachurin, A. M., Zhang, L., Yu, L., and Deisenhofer, J. (1998) *Proc. Natl. Acad. Sci. U.S.A.* 95, 8026–8033.
98. Hunte, C., Koepke, J., Lange, C., Rossmanith, T., and Michel, H. (2000) *Struct. Fold. Des.* 8, 669–684.
99. Crofts, A. R., and Wang, Z. (1989) *Photosynth. Res.* 22, 69–87.
100. Engstrom, G., Xiao, K., Yu, C. A., Yu, L., Durham, B., and Millett, F. (2002) *J. Biol. Chem.* (in press).
101. Lang, C., and Hunte, C. (2002) *Proc. Natl. Acad. Sci. U.S.A.* 99, 2800–2805.

B10262956